Electronic Supplementary Material (ESI) for Materials Advances.
This journal is © The Royal Society of Chemistry 2024

Histidine-functionalized ROS scavenging hybrid nanozyme for therapeutic application in Parkinson's disease pathogenesis

Sanjay Prasad‡, Parthsarathi Nayak‡ and Patrick D'Silva*

Department of Biochemistry and Inorganic & Physical Chemistry, Indian Institute of Science, Bangalore- 560012 (India)
[*] Email: Patrick@iisc.ac.in
[‡] These authors contributed equally to this work

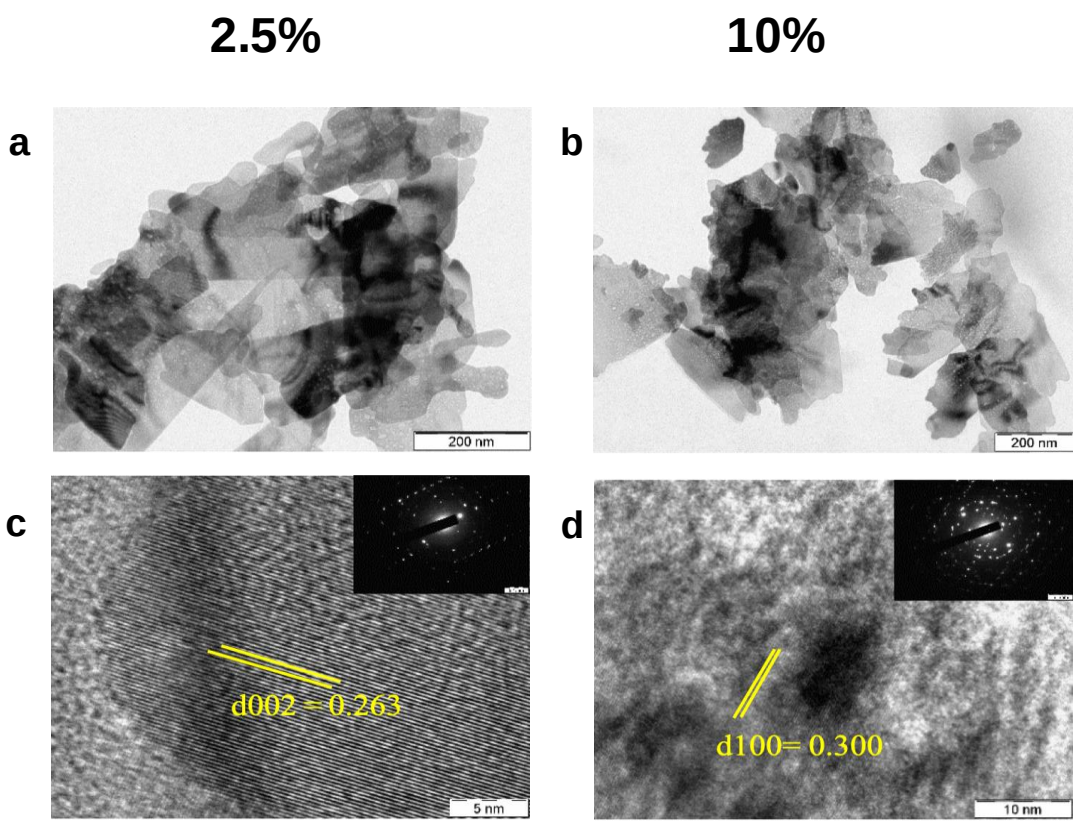

Figure S1. TEM and HR-TEM characterization of different amounts of Cu (2.5% and 10%) doped ZnO. (a & b) TEM analysis. (c & d) HR-TEM analysis. The selected area electron diffraction inset in the HR-TEM images. The reduction of d-spacing in NPs is attributed to the doping of Cu in Cu-doped ZnNPs.

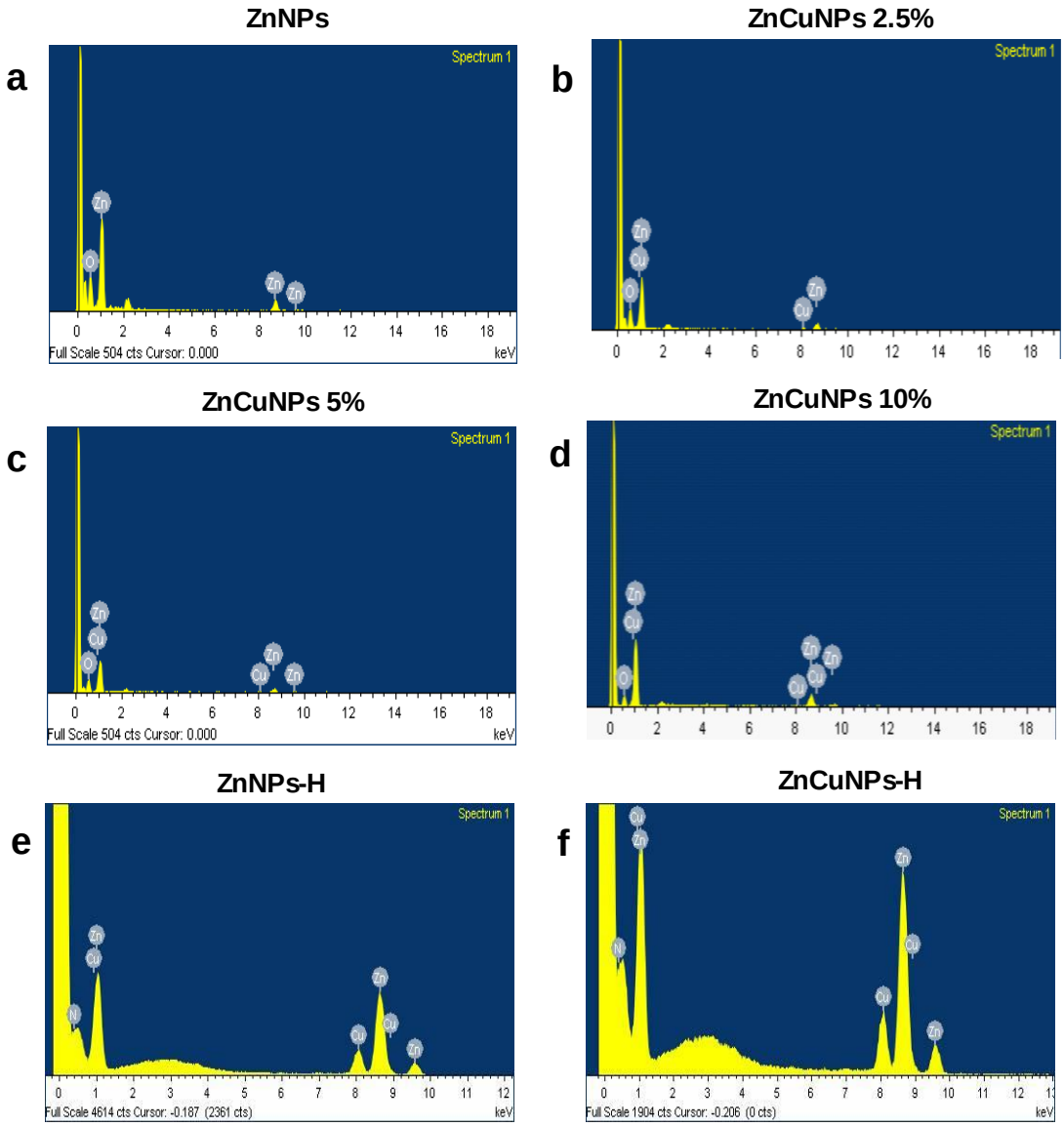

Figure S2. EDX analysis of NPs. (a) ZnNPs. (b) ZnCuNPs-2.5%. (c) ZnCuNPs-5%. (d) ZnCuNPs-10%. (e) ZnNPs-H. (f) ZnCuNPs-H.

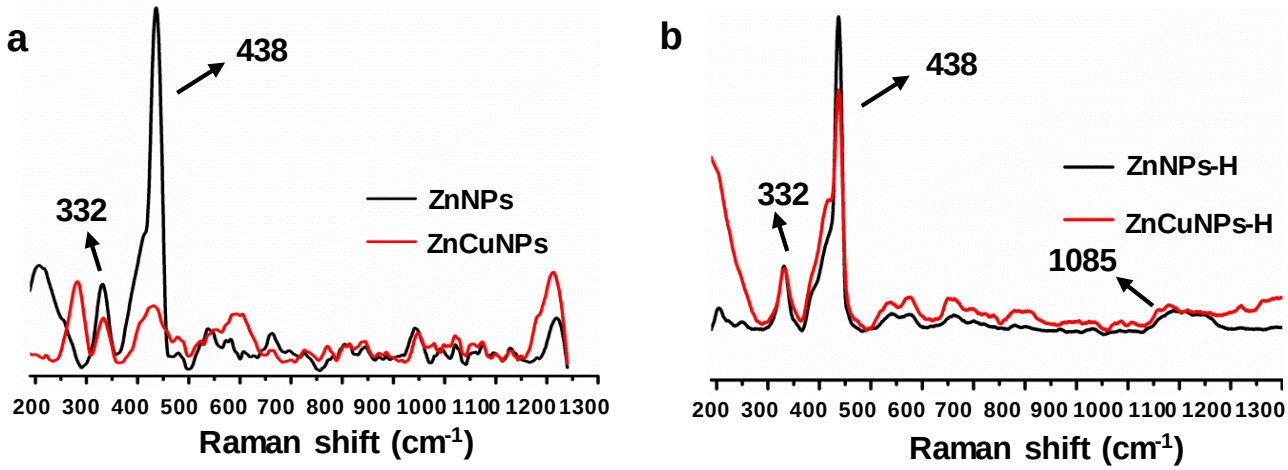

Figure S3. Raman characterization of NPs. (a) Raman Spectra showing the characteristic peak at 438 cm^{-1} is assigned to the vibration of oxygen atoms in ZnNPs and ZnCuNPs. (b) Raman Spectra showing the characteristic peak 1085 cm^{-1} is assigned to N-H band of histidine in addition to 438 cm^{-1} of ZnNPs.

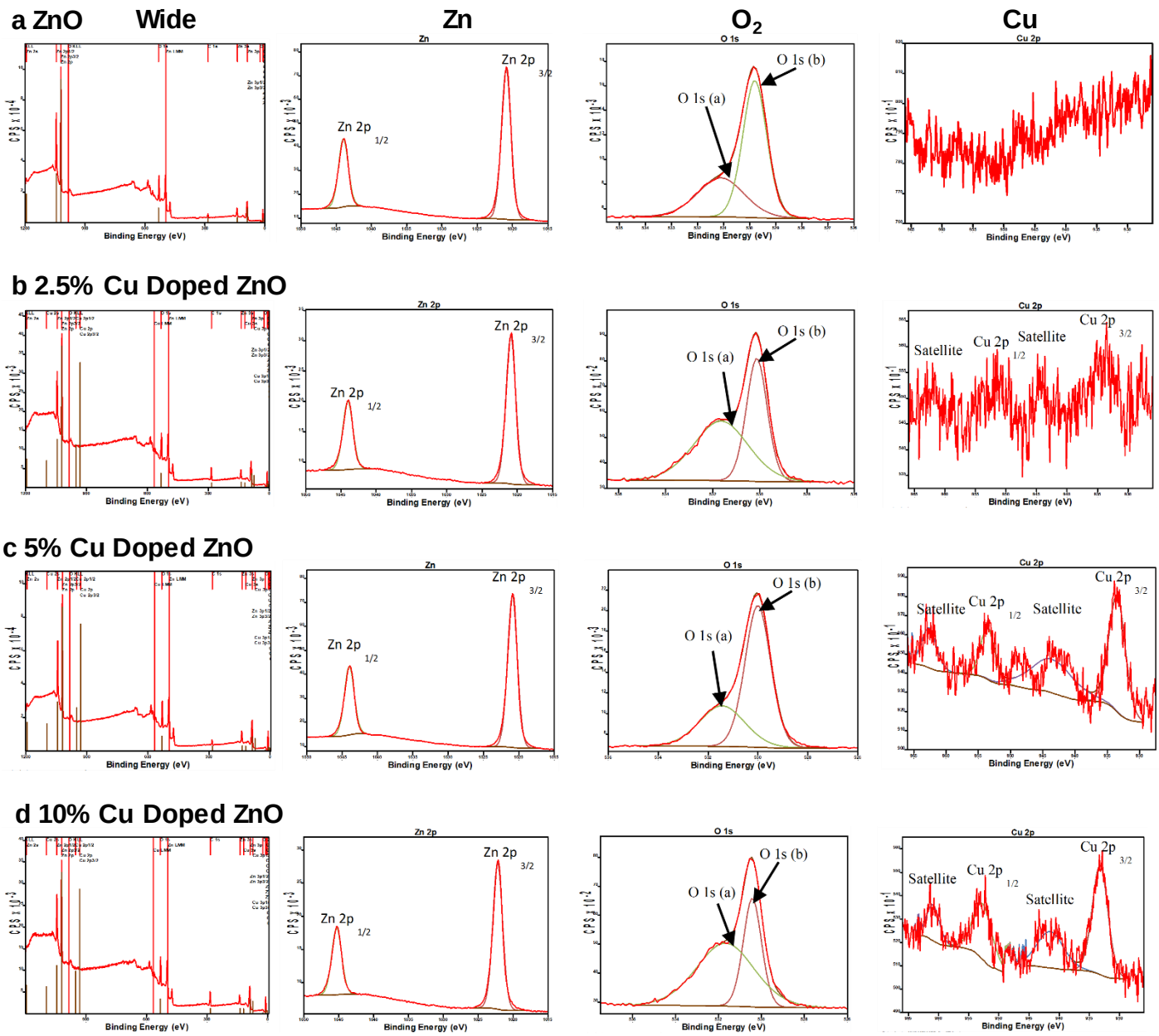

Figure S4. XPS analysis. (a) ZnNPs. (b) 2.5% Cu-doped ZnNPs. (c) 5% Cu-doped ZnNPs. (d) 10% Cu-doped ZnNPs. 4th column shows Cu peaks in Cu-doped ZnNP; no Cu peaks were visible in pure ZnNPs, confirming the doping. Other columns show their respective components and prove the presence of zinc, oxygen, and copper in the NPs. CasaXPS software was used for data processing.

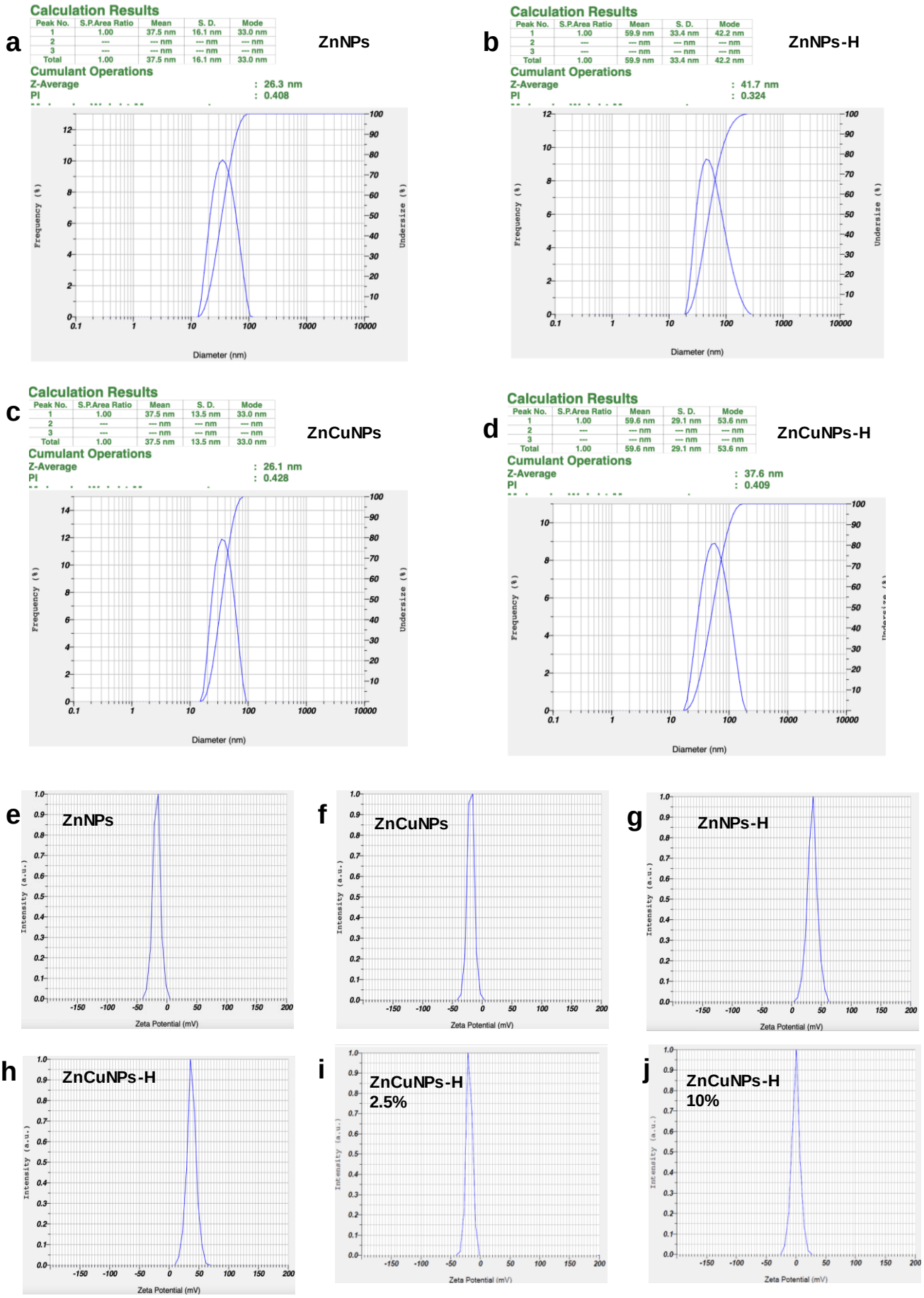

Figure S5. Hydrodynamic size analysis. (a) ZnNPs, (b) ZnNPs-H, (c) ZnCuNPs and (d) ZnCuNPs-H. Surface potential analysis of (e) ZnNPs, (f) ZnCuNPs, (g) ZnNPs-H, (h) ZnCuNPs-H, (i) ZnCuNPs-H (Cu 2.5% doping with ZnNPs). (j) ZnCuNPs-H (Cu 10% doping with ZnNPs). Determined by particle charge analyzer. (HORIBA Scientific Nanopartica SZ-100V2)

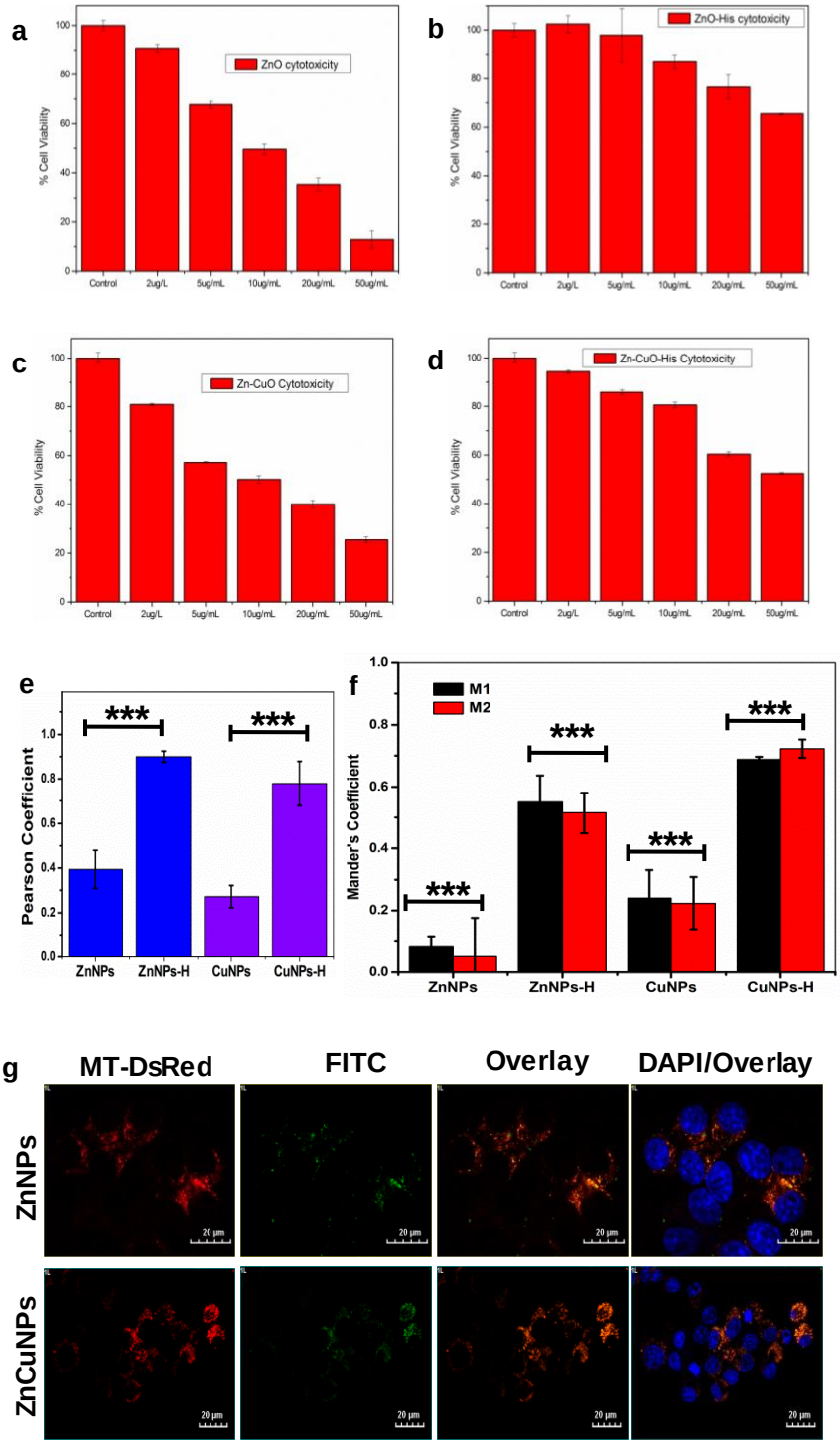

Figure S6. Cytotoxicity and co-localization of NPs. Cytotoxic profile of dose-dependent (a) ZnNPs. (b) ZnNPs-H. (c) ZnCuNPs. (d) ZnCuNPs-H. (e) Pearson's correlation coefficient of mitochondrial-specific NPs co-localization (fig. 5c). (f) Distribution of M1 (fraction of mitochondria in NPs area) and M2 (fraction of NPs in mitochondrial area) co-occurrence coefficient. (g) ZnNPs/ZnCuNPs tagged FITC localization tracked upon N2A cells stained with DAPI and transfected with MTS-DsRed specific to mitochondria. The error bar indicates ±S.E.M. of three independent experiments with respective significance values, *: p <0.05; **: p < 0.01; ***: p<0.001, compared to the control.

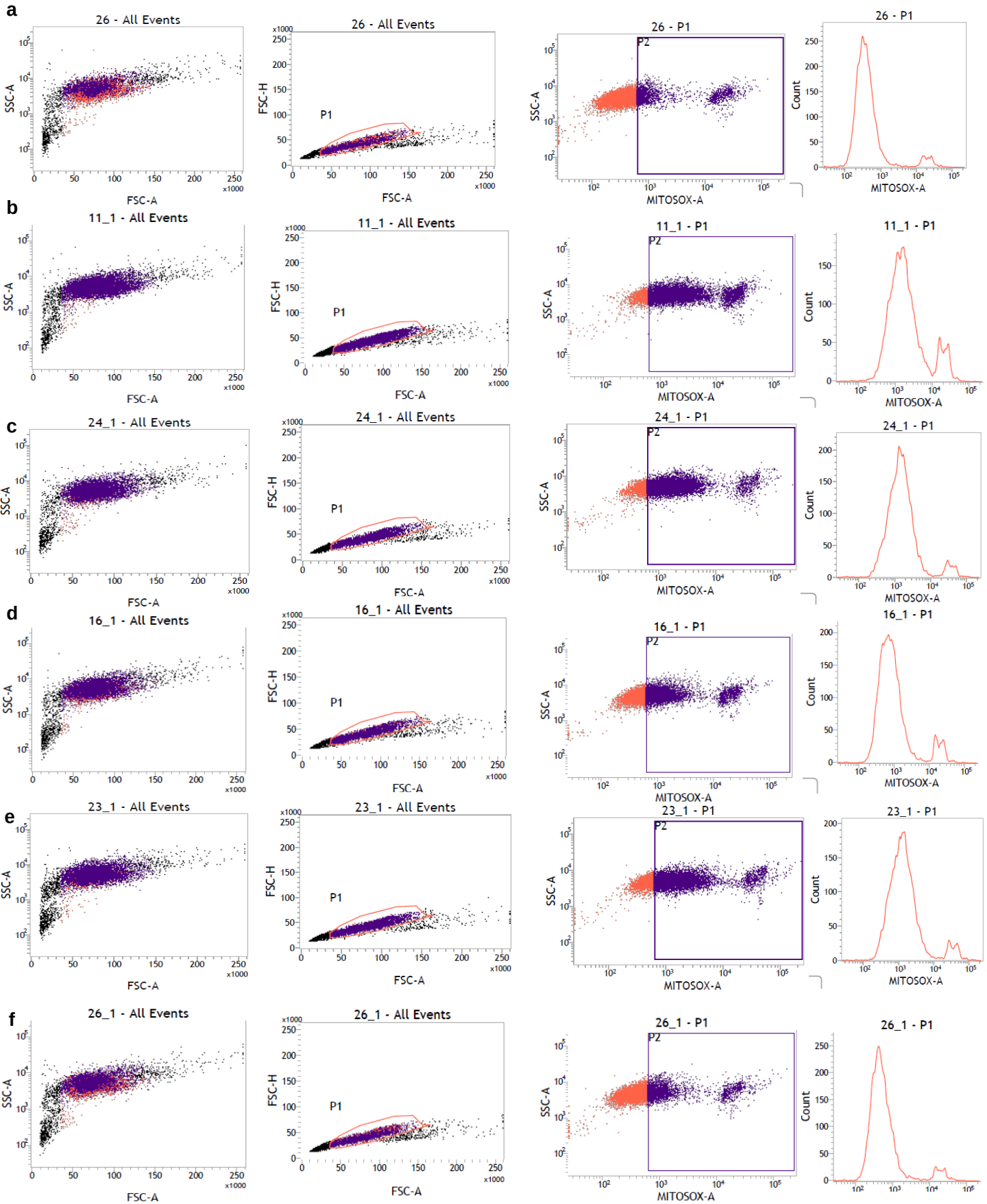

Figure S7. Fluorescence scatter plot and histogram data observed from flow cytometric analysis of MitoSOX treated cells upon elevation of superoxide by rotenone. (a) Control (Only cells). (b) Rotenone treated cells (in the absence of NPs). (c) Rotenone treated cells with ZnNPs. (d) Rotenone treated cells with ZnNPs-H. (e) Rotenone treated cells with ZnCuNPs. (f) Rotenone treated cells with ZnCuNPs-H.

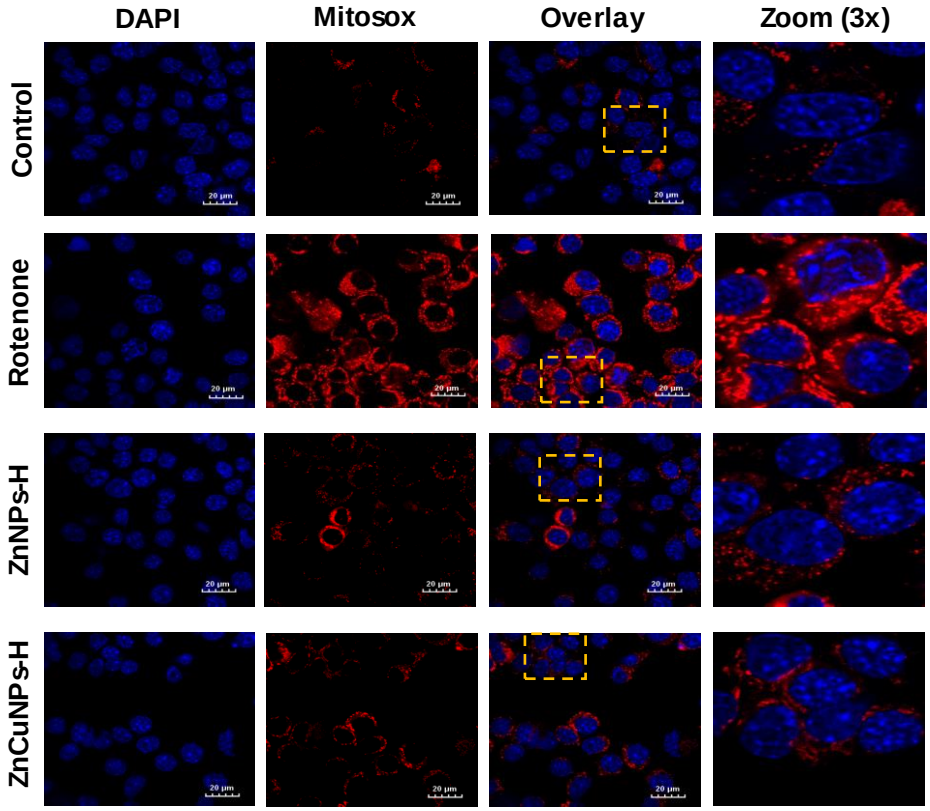

Figure S8. Superoxide scavenging activity of Nanozyme. Cytoprotective effect of functionalized and non-functionalized ZnNPs/ ZnCuNPs in N2a cells upon elevation of superoxide by rotenone stained with DAPI and MitoSOX analyzed by Confocal microscopy. The error bar indicates ± S.E.M. of three independent experiments with respective significance value, *: $p < 0.05$; **: $p < 0.01$; ***: $p < 0.001$, compared to control.

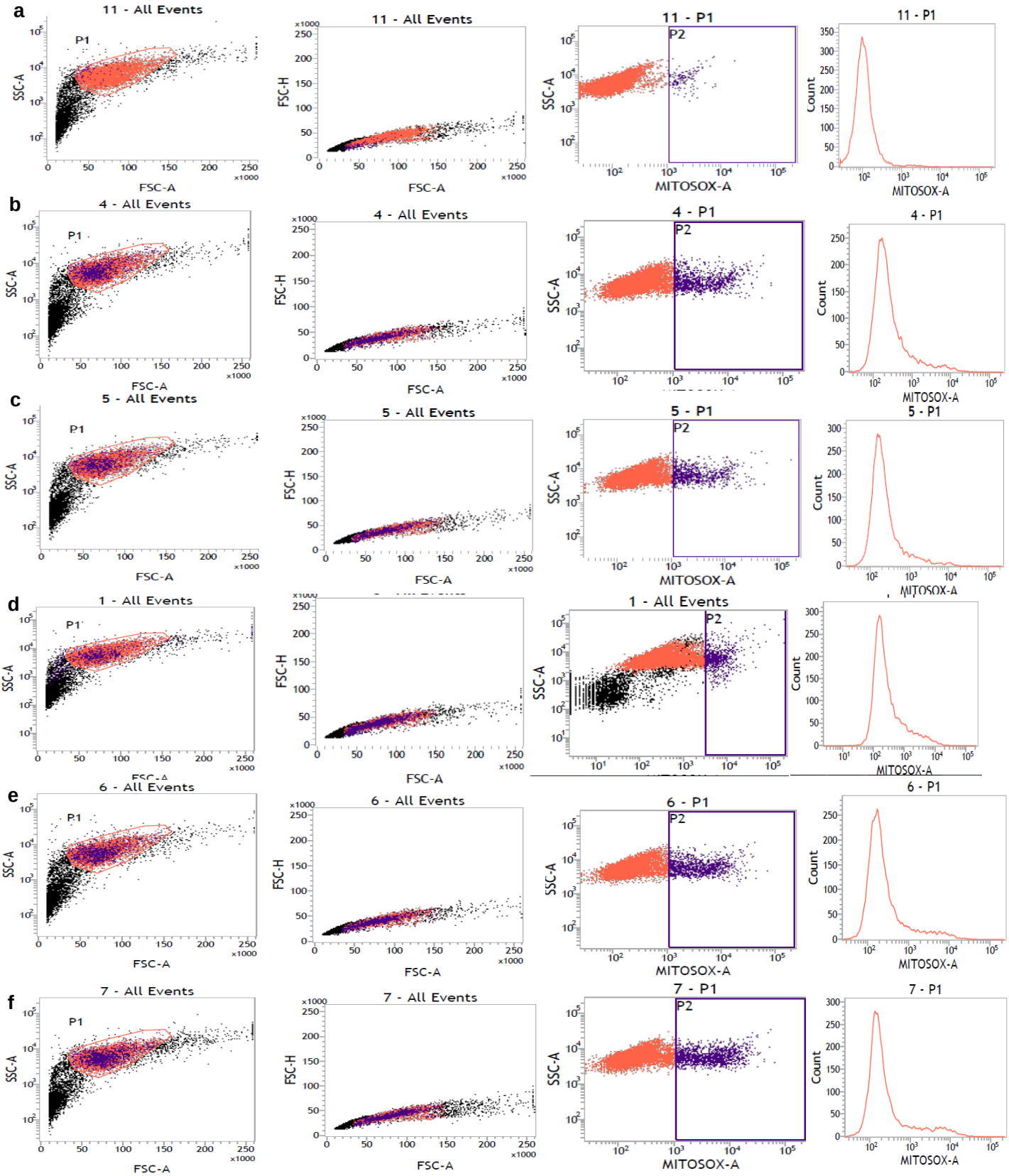

Figure S9. Fluorescence scatter plot and histogram data observed from flow cytometric analysis of MitoSOX treated cells upon elevation of superoxide by LCS-1. (a) Control (Only cells). (b) LCS-1 treated cells (in absence of NPs). (c) LCS-1 treated cells with ZnNPs. (d) LCS-1 treated cells with ZnNPs-H. (e) LCS-1 treated cells with ZnCuNPs. (f) LCS-1 treated cells with ZnCuNPs-H

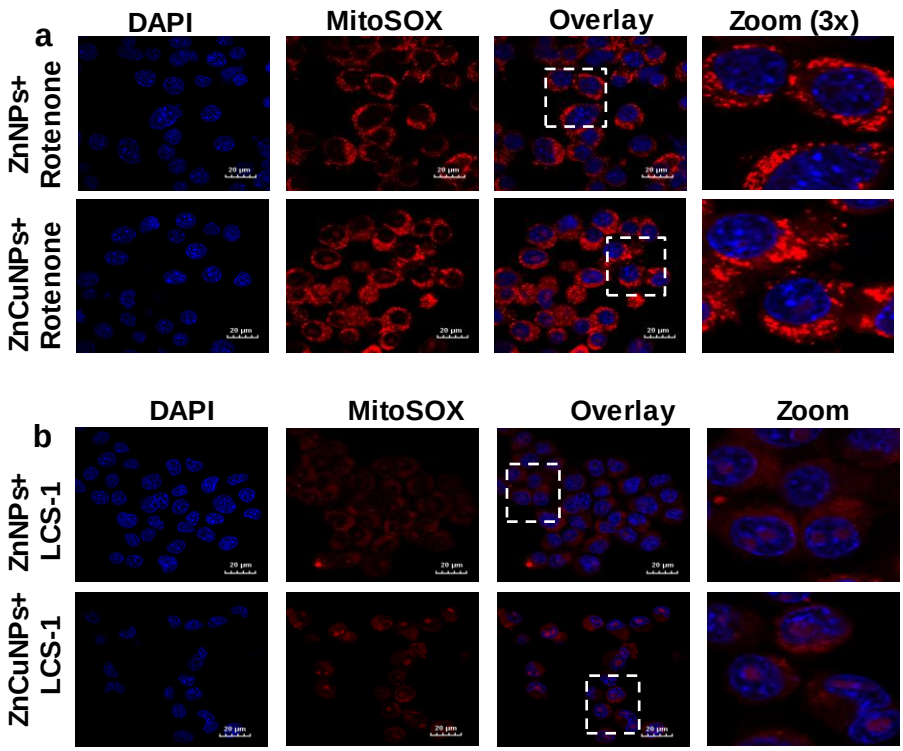

Figure S10. ROS scavenging activity of ZnNPs and ZnCuNPs in N2a cells stained with DAPI and MitoSOX analyzed by confocal microscopy in the presence of (a) rotenone. (b) LCS-1 (Scale bar is 20 mm).

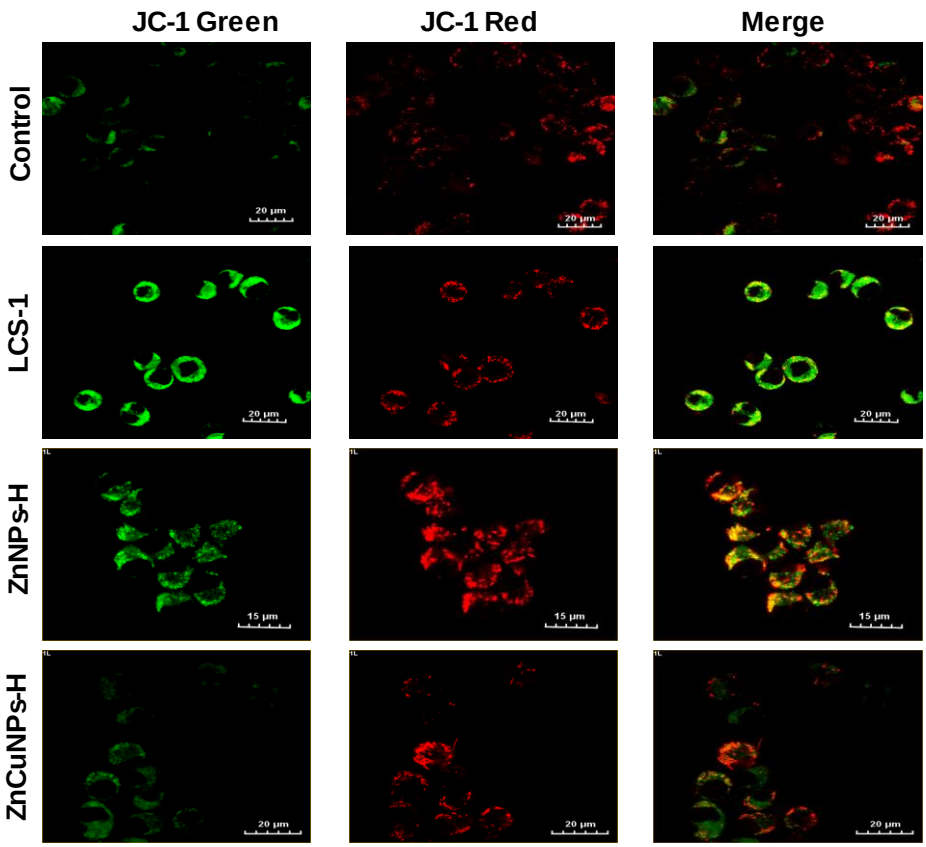

Figure S11. Effect of LCS-1 on mitochondrial health. Confocal microscopic analysis of mitochondrial membrane potential of functionalized NPs treated cells using JC-1 dye in the absence and presence of LCS-1 (Scale bar is 20 mm).

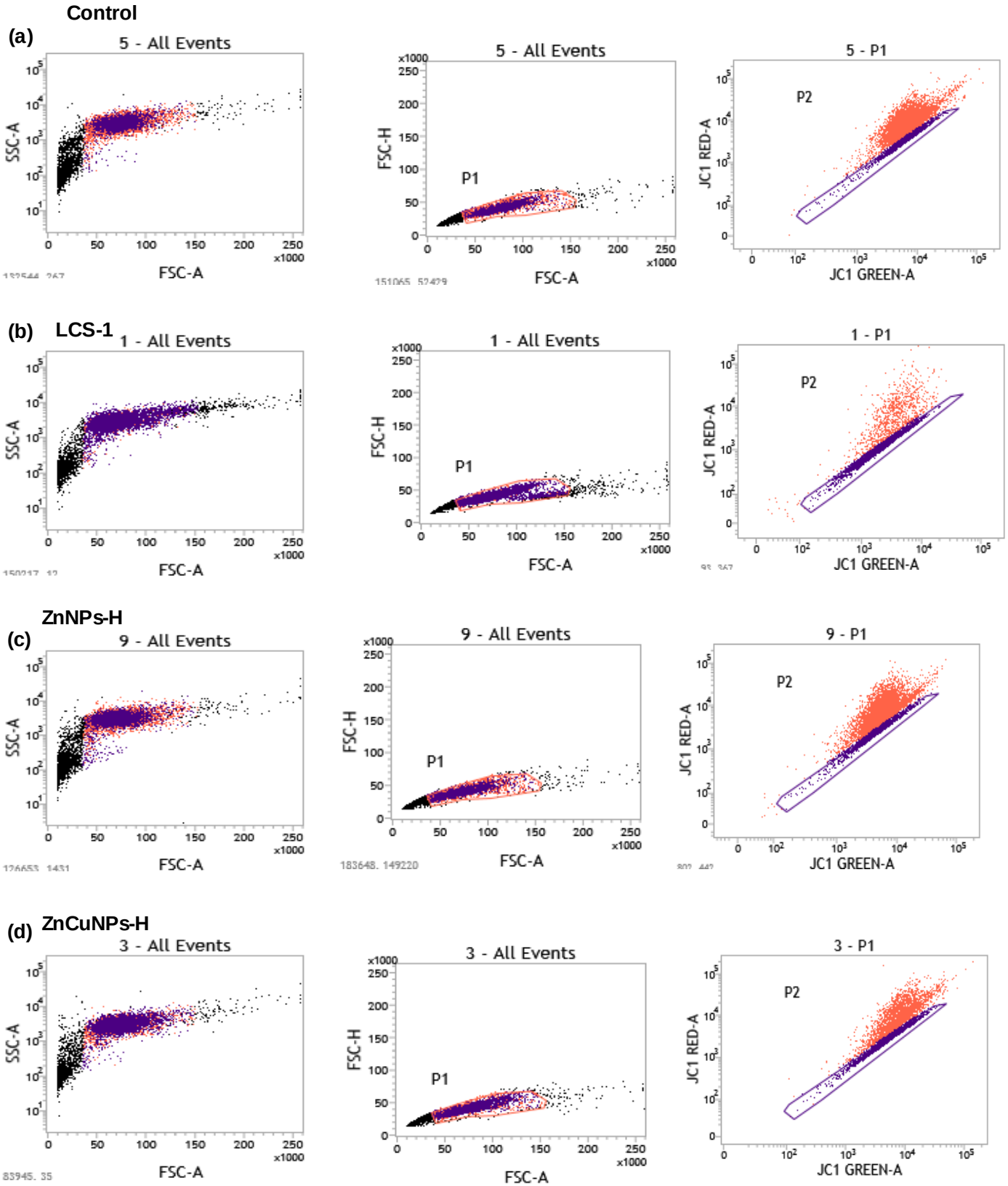

Figure S12. Flow cytometric analysis. Fluorescence scatter plot showing mitochondrial membrane potential using JC-1 dye in the absence and presence of LCS-1 treated cells (a) Control (without LCS-1 and NPs). (b) LCS-1 only, (c) ZnNPs-H. (d) ZnCuNPs .

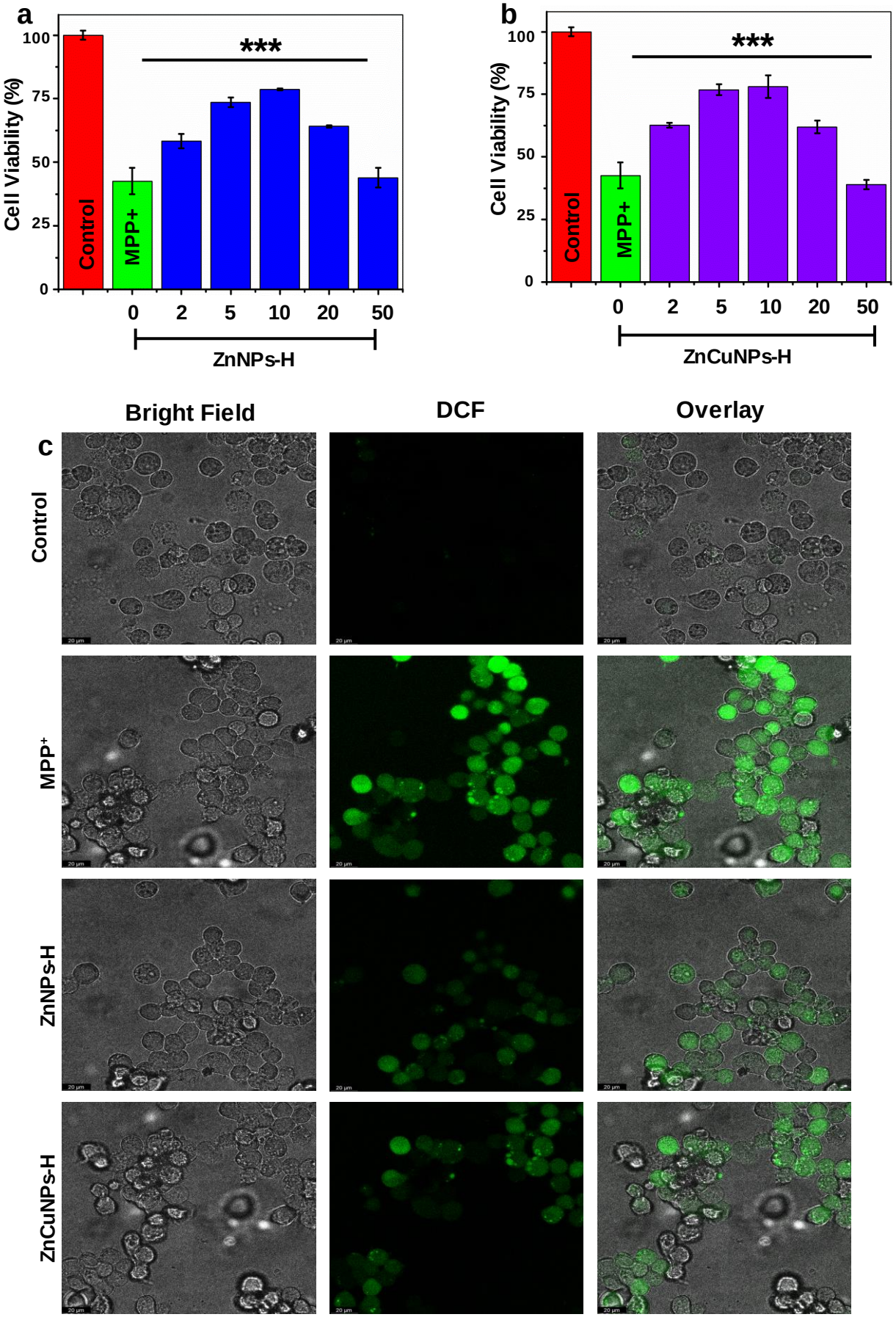

Figure S13. Functionalized NPs showed antioxidant potential against oxidative stress induced by MPP^+. Cytoprotective role of (a) ZnNPs-H. (b) ZnCuNPs-H. (c) Fluorescent photomicrograph of N2a cells treated with MPP^+ stained with DCFH-DA showing intracellular ROS L (Scale is 20 mm).

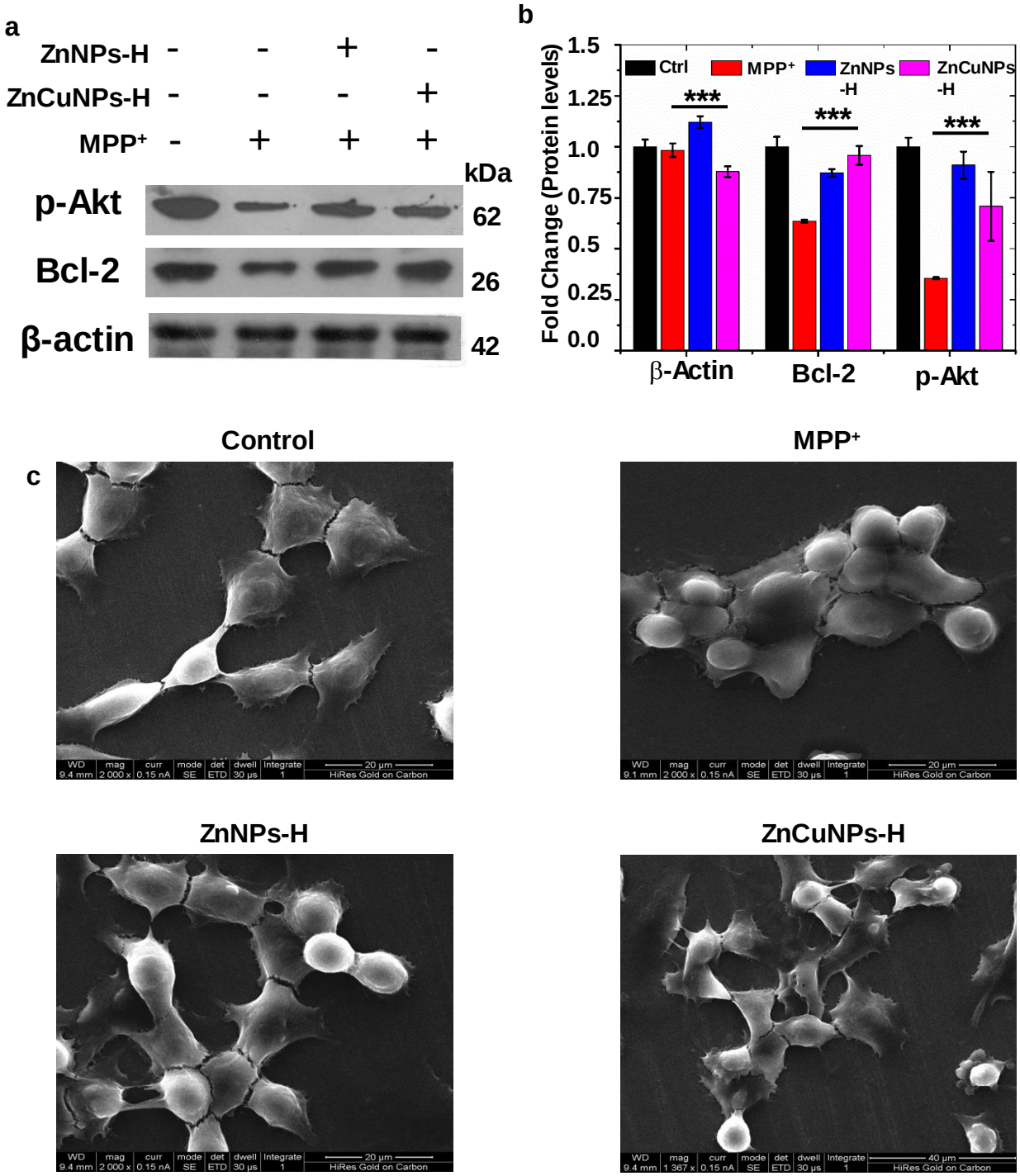

Figure 14. (a) & (b) Western Blot analysis (the protein bands were quantified using Multi Gauge V3.0) and (c) SEM representative micrographs of N2a cells challenged with MPP^+. Control (MPP^+ untreated cells), MPP^+ only, ZnNPs-H treated and ZnCuNPs treated cells.